Theory of structures in near-electrode plasma regions

M. S. Benilov
*Arbeitsgemeinschaft Plasmaphysik, Ruhr-University Bochum, Postfach 102148, D-4630 Bochum 1, Germany**
(Received 19 August 1991)

A number of well-known features of a constricted discharge in plasma near-electrode layers (e.g., the normal current-density effect) proceeds from the fact that the layer thickness is much smaller than longitudinal dimensions. A better understanding of these features may be achieved by means of the asymptotic approach, which treats the ratio of the above-mentioned lengths as a small parameter. In the vicinity of extreme points of the current-voltage characteristic of the distributed discharge regime (regime with a uniform distribution of the current density over the electrode surface), this approach is similar to the perturbation method, reducing the reaction-diffusion equations in the vicinity of an instability point to the Ginzburg-Landau equation, and results in a Fisher-type equation for perturbations of current-density distribution. Using this equation, stationary perturbations are found and their stability is analyzed. In addition, the above-noted asymptotic approach is applied to the analysis of normal current-density regimes. In particular, it is shown that interaction of a current spot (covered area) with lateral boundaries and/or other spots is transmitted by means of the exponentially small perturbations introduced by spots into regions occupied by the cold and hot phases. Application of the results obtained to the transition between the normal and abnormal regimes of the glow-discharge near-cathode region is discussed.

PACS number(s): 52.40.Hf, 52.80.Hc

I. INTRODUCTION

The appearance of current structures in plasma near-electrode layers presents an important example of a self-organization phenomenon; see, e.g., [1–10]. Most theoretical investigations of these structures (for instance, [3,4,7,8]) are based on a phenomenological equation for the current-density distribution across the electrode surface. This approach results in interesting static and dynamic patterns. On the other hand, it seems worth trying to develop a technique of investigation of the structures on a physical basis, i.e., in the framework of some physical model describing the basic physics of the particular problem.

The specifics of current structures in near-electrode layers that distinguish them from other dissipative structures proceeds from the fact that the thickness of a near-electrode layer is usually much less than its longitudinal dimensions. It is this inequality that plays a fundamental role in such well-known effects as the normal current-density effect or the appearance on an electrode surface of current spots (covered areas) whose radius is much less than longitudinal dimensions. Thus an appropriate way to investigate near-electrode current structures is to treat the basic (three-dimensional) physical model asymptotically, taking advantage of the smallness of the ratio of the above-mentioned length scales.

Such an approach is developed in the present paper. Basically, two questions are studied. First, the question of intermediate stationary regimes between regimes with spots and the distributed regime is discussed: whether such regimes exist; if so, whether they are stable and what their properties are.

Second the question of an interaction of a current spot (covered area) with lateral boundaries of the discharge vessel and/or with other spots is discussed. This interaction is of principal importance for existence of these structures. Indeed, each spot, which is an element of a regular structure, can sense positions of neighboring spots and lateral boundaries; the correlation between the shape of the covered area on the cathode of the normal glow discharge and the shape of the cathode may be referred to as the well-known example. However, the way in which this interaction is transmitted through the near-electrode region occupied by the cold phase and how to calculate it are not well understood.

In Sec. II the problem is stated and the general behavior of solutions is discussed. An equation governing perturbations of the current-density distribution along the electrode surface in the vicinity of extreme points of the distributed discharge current-voltage characteristic is asymptotically derived in Sec. III. Stationary solutions to this equation are found analytically in Sec. IV for the planar case, and numerically in Sec. V for the axisymmetric case. Some considerations for the general case are presented and stability of the stationary solutions is discussed in Sec. VI. Asymptotic analysis of normal regimes of current transfer (regimes with coexistence of phases) is presented in Sec. VII. Finally, in Sec. VIII among other concluding remarks the application of obtained results to the glow-discharge cathode region is discussed.

II. THE STATEMENT OF THE PROBLEM

A. The model

Consider current transfer through a plasma near-electrode layer (Fig. 1). The discharge vessel is in the form of the cylinder whose cross section is not necessarily circular, the lateral surface of the cylinder being insulat-

ing, the foot being the electrode surface. The x and z axes of the Cartesian coordinate system are parallel to the electrode surface, the y axis is directed into plasma volume. We treat a class of models of current transfer through the near-electrode region which can be described by a system of reaction-diffusion differential equations

$$\mathbf{A}\frac{\partial \mathbf{X}}{\partial t}=\mathbf{B}+\nabla\cdot(\mathbf{D}\nabla\mathbf{X}) . \tag{1}$$

Here the vector $\mathbf{X}$ represents a set of functions to be found describing space distributions of plasma parameters in the near-electrode region; the vector $\mathbf{B}$ and the matrices $\mathbf{A}$ and $\mathbf{D}$ will be treated as arbitrary prescribed functions of the components of the vector $\mathbf{X}$; t designates time.

Consider, for instance, the well-known hydrodynamical set of equations describing distributions of concentrations of ions and electrons n_i and n_e and the potential φ in the near-cathode space-charge layer of the glow discharge

$$\frac{\partial n_i}{\partial t}+\operatorname{div}(-D_i \operatorname{grad} n_i-\mu_i n_i \operatorname{grad}\varphi)=w , \tag{2}$$

$$\frac{\partial n_e}{\partial t}+\operatorname{div}(-D_e \operatorname{grad} n_e+\mu_e n_e \operatorname{grad}\varphi)=w , \tag{3}$$

$$\epsilon_0 \operatorname{div}(\operatorname{grad}\varphi)=e(n_e-n_i) , \tag{4}$$

where D_i, D_e, μ_i, and μ_e are diffusion coefficients and mobilities of ions and electrons (prescribed functions of the electric field strength $|\operatorname{grad}\varphi|$); w is the rate of change of the concentrations of ions and electrons due to volume ionization and recombination (a prescribed function of n_i, n_e, and $|\operatorname{grad}\varphi|$); ϵ_0 is the permittivity of the free space; e is the electronic charge. These equations assume the form (1), if

$$\mathbf{X}=\begin{vmatrix} n_i \\ n_e \\ \varphi \end{vmatrix}, \quad \mathbf{B}=\begin{vmatrix} w \\ w \\ e(n_i-n_e) \end{vmatrix},$$
$$\mathbf{A}=\begin{vmatrix} 1 & 0 & 0 \\ 0 & 1 & 0 \\ 0 & 0 & 0 \end{vmatrix}, \quad \mathbf{D}=\begin{vmatrix} D_i & 0 & \mu_i n_i \\ 0 & D_e & -\mu_e n_e \\ 0 & 0 & \epsilon_0 \end{vmatrix} . \tag{5}$$

To make use of the fact that the characteristic dimension L of the cross section of the discharge vessel is usually much greater than the characteristic thickness of the near-electrode layer h, we normalize the coordinates x and z by L, the coordinate y by h, and the time by t^0, which is the characteristic time of relaxation of the system. Splitting derivatives in y and in x,z we rewrite (1) as

$$\mathbf{A}\frac{\partial \mathbf{X}}{\partial \tilde{t}}=\tilde{\mathbf{B}}+(\tilde{\mathbf{D}}\mathbf{X}')'+\chi\nabla_{\parallel}\cdot(\tilde{\mathbf{D}}\nabla_{\parallel}\mathbf{X}) , \tag{6}$$

where $\tilde{t}=t/t^0$; $\tilde{\mathbf{B}}=t^0\mathbf{B}$; $\tilde{\mathbf{D}}=t^0\mathbf{D}/h^2$; a prime designates differentiating in $\tilde{y}=y/h$; $\nabla_{\parallel}$ is the gradient in the variables $\tilde{x}=x/L$ and $\tilde{z}=z/L$; $\chi=h^2/L^2$. The tilde will be dropped in future for the sake of brevity.

Suppose that the system (6) is supplemented with appropriate boundary conditions which include conditions at $y=0$ (these conditions should account for basic physical processes on the electrode surface), at large values of y (these conditions follow from the requirement that far away from the electrode surface the considered solution should become the solution corresponding to the plasma column), and conditions on the lateral surface of the vessel. The explicit form of these boundary conditions is not important for the following analysis, we assume only that one of these conditions specifies the voltage drop U across the considered near-electrode region, this voltage drop being constant along the electrode surface, and that these conditions allow the existence of a stationary one-dimensional solution $\mathbf{X}=\mathbf{X}^{(1)}(y)$ to the whole problem. The first assumption holds if the voltage drop in the near-electrode region is much greater than that in the adjacent plasma, which is usually the case. The second assumption means, in particular, that the nonuniformity of the electrode surface is negligible.

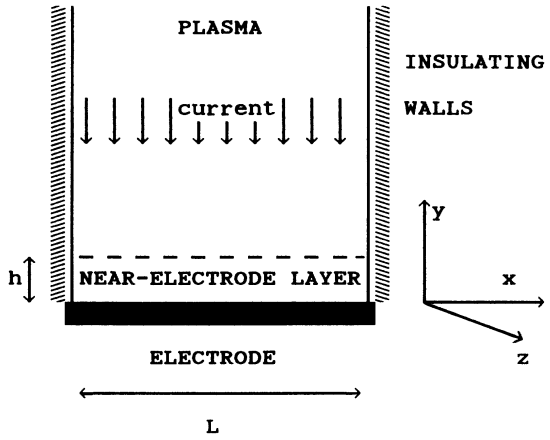

FIG. 1. Geometry of the problem.

B. General behavior of stationary solutions

The above-mentioned stationary one-dimensional solution $\mathbf{X}^{(1)}(y)$ describes a regime in which the current density is constant along the electrode surface (regime of distributed current transfer). Assume that the current-voltage characteristic $U(I)$ described by this solution is N shaped (the line OAMBN in Fig. 2).

Non-one-dimensional solutions to the considered problem $\mathbf{X}=\mathbf{X}(x,y,z)$ describe regimes with current density variable along the electrode surface (regimes of constricted current transfer). The general impression of these solutions is given by the two-dimensional numerical calculations [11] (these calculations were carried out in the framework of a thermal constriction model). A representative current-voltage characteristic is shown schematically in Fig. 2 by the line CDEF. As the ratio of the dimension in the direction normal to the electrode surface to the along-surface dimension becomes smaller, the bifurcation points C and F (in these points the non-one-dimensional solution joins the one-dimensional solution) come nearer to the points of maximum and minimum A

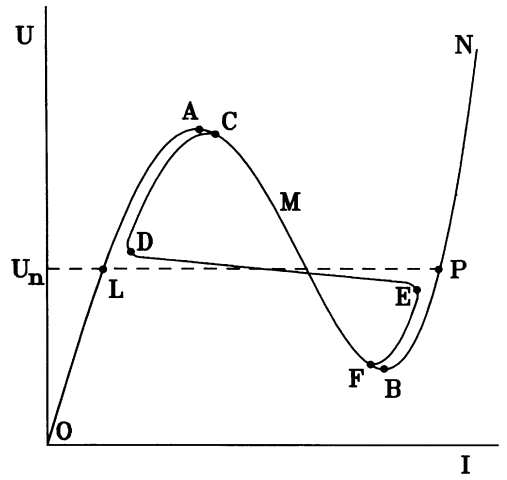

FIG. 2. Schematic of the current-voltage characteristics.

and B of the one-dimensional current-voltage characteristic; the section DE becomes closer to the horizontal line $U=U_n$ (U_n is a certain value which does not depend on the along-surface dimension); the sections CD and EF become closer to the sections AL and PB.

The distribution of the current density over the electrode surface evolves along the current-voltage characteristic $CDEF$ as follows. At point C the uniformity of this distribution is broken and a hot domain surrounded by a cold phase (that is, a certain small region with the current density higher than in an adjacent zone; in other words, a narrow current spot) begins forming. On the section CD the current density in this domain increases to a value corresponding to the point P of the one-dimensional current-voltage characteristic; the current density in the region occupied by the cold phase falls to a value corresponding to the point L. On the section DE the hot phase spreads along the electrode surface, the current densities in the regions occupied by the hot and cold phases being nearly constant (regimes with coexistence of phases or normal regimes, U_n being the normal voltage drop). At point E the hot phase occupies the whole electrode surface except a certain small region (a cold domain). Section EF is similar to CD; the cold domain vanishes gradually on this section and the current distribution becomes uniform again.

The theory developed in Secs. III–VI provides description of non-one-dimensional solutions in the vicinity of extreme points of the one-dimensional current-voltage characteristic A and B. In Sec. VII a solution describing section DE is studied.

III. EQUATION FOR PERTURBATIONS OF THE CURRENT-DENSITY DISTRIBUTION IN THE VICINITY OF EXTREME POINTS

Suppose $\chi\to 0$, with the number of non-one-dimensional solutions under consideration being fixed. The last supposition means that those non-one-dimensional solutions are considered which branch off from the one-dimensional solution with wavelengths in x and z directions comparable with the vessel transverse length scale L. We seek these non-one-dimensional solutions in the vicinity of the extreme point, say, point of minimum B [this vicinity is specified as $(U-U_B)/U_B=O(\chi^2)$] as the series

$$\mathbf{X}=\mathbf{X}_B(y)+\chi\mathbf{X}_1(x,y,z,\tau)+\chi^2\mathbf{X}_2(x,y,z,\tau)+\cdots , \quad (7)$$

where $\tau=\chi t$, $\mathbf{X}_B(y)$ designates the solution $\mathbf{X}^{(1)}(y)$ in point B.

Substituting this series in (6) and expanding in powers of χ one obtains the equations governing the functions $\mathbf{X}_1$, $\mathbf{X}_2$:

$$\mathbf{B}_1\mathbf{X}_1+(\mathbf{D}_B\mathbf{X}_1'+\mathbf{D}_1\mathbf{X}_1\mathbf{X}_B')'=0 , \quad (8)$$

$$\mathbf{A}_B\frac{\partial\mathbf{X}_1}{\partial\tau}=\mathbf{B}_1\mathbf{X}_2+\mathbf{B}_2\mathbf{X}_1\mathbf{X}_1 +(\mathbf{D}_B\mathbf{X}_2'+\mathbf{D}_1\mathbf{X}_2\mathbf{X}_B'+\mathbf{D}_1\mathbf{X}_1\mathbf{X}_1'+\mathbf{D}_2\mathbf{X}_1\mathbf{X}_1\mathbf{X}_B')' +\mathbf{D}_B\Delta_{\|}\mathbf{X}_1 , \quad (9)$$

where $\Delta_{\|}=\nabla_{\|}^2$; matrices $\mathbf{A}_B$, $\mathbf{B}_1$, $\mathbf{B}_2$, $\mathbf{D}_B$, $\mathbf{D}_1$ and $\mathbf{D}_2$ are (dependence on $|\mathrm{grad}\mathbf{X}|$ is neglected for brevity)

$$\begin{aligned}
&\mathbf{A}_B=\mathbf{A}(\mathbf{X}_B),\quad (\mathbf{B}_1)_{ij}=\frac{\partial\mathbf{B}_i}{\partial\mathbf{X}_j}(\mathbf{X}_B) ,\\
&(\mathbf{B}_2)_{ijk}=\frac{1}{2}\frac{\partial^2 B_i}{\partial X_j\partial X_k}(\mathbf{X}_B) ,\\
&\mathbf{D}_B=\mathbf{D}(\mathbf{X}_B),\quad (\mathbf{D}_1)_{ijk}=\frac{\partial D_{ij}}{\partial X_k}(\mathbf{X}_B) ,\\
&(\mathbf{D}_2)_{ijkm}=\frac{1}{2}\frac{\partial^2 D_{ij}}{\partial X_k\partial X_m}(\mathbf{X}_B) .
\end{aligned} \quad (10)$$

We shall imply that Eqs. (8) and (9) are considered along with corresponding boundary conditions which are obtained by similar expanding of the boundary conditions mentioned in Sec. II. Boundary conditions for Eq. (8) are linear and homogeneous, as well as the equation itself. Equation (9) is also linear but inhomogeneous (some terms involve $\mathbf{X}_1$ and do not involve $\mathbf{X}_2$). The same is valid for boundary conditions for this equation; in addition, one of these conditions contains an inhomogeneous term proportional to $(U-U_B)$.

The existence of a nontrivial solution to the uniform homogeneous problem (8) follows from the fact that point B is the extreme point of the one-dimensional stationary current-voltage characteristic. This solution may be written as

$$\mathbf{X}_1=Z(y)F(x,z,\tau),\quad \mathbf{Z}(y)=\left[\frac{\partial\mathbf{X}^{(1)}}{\partial I}\right]_B , \quad (11)$$

where $Z(y)$ designates the derivative of the solution $\mathbf{X}^{(1)}$ with respect to current I at point B, and $F(x,z,\tau)$ is some scalar dimensionless function yet to be specified.

Now Eq. (9) may be rewritten as

$$\mathbf{B}_1\mathbf{X}_2+(\mathbf{D}_B\mathbf{X}_2'+\mathbf{D}_1\mathbf{X}_2\mathbf{X}_B')' = \frac{\partial F}{\partial\tau}\mathbf{A}_B\mathbf{Z}-\Delta_{\|}F\mathbf{D}_B\mathbf{Z}-F^2[\mathbf{B}_2\mathbf{Z}\mathbf{Z}+(\mathbf{D}_1\mathbf{Z}\mathbf{Z}'+\mathbf{D}_2\mathbf{Z}\mathbf{Z}\mathbf{X}_B')'] . \quad (12)$$

Equation (12) (we imply again that it is considered along with corresponding boundary conditions) represents a linear inhomogeneous problem, the corresponding homogeneous problem being Eq. (8). The existence of a nontrivial solution to (8) means that for the problem (12) to be solvable its right-hand side should satisfy some special condition, namely, it should be orthogonal to the solution $\mathbf{Z}^*(y)$ of the linear homogeneous problem which is adjoint to (8) (e.g., Coddington and Levinson [12]). By inspecting the general structure of (12) one can see that this solvability condition assumes the following form (with the accuracy of constant coefficients of the order of unity which can be absorbed by renormalization of F,τ):

$$\frac{\partial F}{\partial\tau}=\Delta_{\|}F-F^2+c^2 . \quad (13)$$

The term c^2, to the accuracy of a coefficient of the order of unity, is equal to $(U-U_B)/(U_B\chi^2)$ and results from the above-mentioned term of one of the boundary conditions that is proportional to $(U-U_B)$.

Evidently, F is proportional to the difference $(j-j_B)$ between the local current density at the electrode surface and the value of the current density corresponding to point B, so this equation may be considered as governing perturbations of the current-density distribution in the vicinity of the extreme point.

It may be desirable to determine numerical values of coefficients of proportionality relating the dimensionless quantities F, c^2, and τ to dimensional $(j-j_B)$, $(U-U_B)$, and time. This task is not much harder than the calculation of the one-dimensional stationary solution alone. Indeed, the main additional element is calculation of the function $\mathbf{Z}^*(y)$; this function is governed by the linear boundary-value problem for the (vector) ordinary differential equation which may be solved by a standard numerical technique, for instance, by that employed in [6].

Equation (13) is studied in biomathematics as the prototype nonlinear equation which admits traveling plane-wave solutions and is usually referred to as the Fisher equation; see, e.g., [13] and references therein. We are interested in stationary solutions of (13) and in their stability. To study stationary solutions it is convenient to introduce the new dependent variable $f=f(x,z)=F/c$. Evidently, there are two constant solutions

$$f=-1, \quad f=1 , \quad (14)$$

corresponding to the one-dimensional stationary solution $\mathbf{X}^{(1)}(y)$ and describing the beginning of the section BM of the one-dimensional current-voltage characteristic and the beginning of the section BN, respectively. Nonconstant solutions $f=f(x,z)$ describe initial sections of the stationary non-one-dimensional solutions branching off from the solution $\mathbf{X}^{(1)}(y)$. In Secs. IV and V these nonconstant solutions are presented for the planar and axisymmetric cases. In Sec. VI some considerations for the general case are presented and stability of stationary solutions is discussed.

Before solving Eq. (13) one should specify boundary conditions for the function F at the boundary of the considered region, that is, at the perimeter of the discharge vessel cross section. These boundary conditions follow from those obeyed by the function $\mathbf{X}$ at the lateral surface of the discharge vessel. For definiteness, assume that the latter are the Neumann (zero derivative) conditions, which are the simplest boundary conditions allowing existence of a one-dimensional solution (the influence of this assumption for the above-considered example of the glow-discharge near-cathode space-charge region is discussed in Sec. VIII). Then the function F also satisfies Neumann conditions.

IV. THE PLANAR CASE

We shall find here stationary nonconstant solutions to (13) in the case when the cross section of the vessel in a rectangle and the function f depends on x only. Evidently, this case corresponds to planar solution of the initial problem: $\mathbf{X}=\mathbf{X}(x,y)$. Supposing the length scale L coincides with the dimension of the rectangle in the direction x, the problem (13) may be treated in the interval [0,1]. Then nonconstant solutions may be written as

$$f=2\sqrt{3}\sin\left[\beta+\frac{2\pi}{3}\right]\frac{1\pm\mathrm{cn}(u\,|m)}{1+\mathrm{dn}(u\,|m)}-2\cos\beta . \quad (15)$$

Here

$$u=2x\left[\frac{c\sin(\beta+\pi/3)}{\sqrt{3}}\right]^{1/2}, \quad m=\frac{\sin(\beta+2\pi/3)}{\sin(\beta+\pi/3)} , \quad (16)$$

$\mathrm{cn}(u\,|m)$ and $\mathrm{dn}(u\,|m)$ are the Jacobian elliptic functions [14], and β is a root of the equation

$$\sqrt{c}=M\Delta , \quad (17)$$

where

$$\Delta=\left[\frac{\sqrt{3}}{\sin(\beta+\pi/3)}\right]^{1/2}K(m) , \quad (18)$$

M is an arbitrary positive integer number, and $K(m)$ is the complete elliptic integral of the first kind [14]. The parameter β satisfies the inequality $0<\beta<\pi/3$.

Solutions described by formula (15) present sequences of alternately rising and falling half waves: the function f grows from the minimum value $f_{\min}=-2\cos\beta$ up to the maximum value $f_{\max}=2\cos(\beta+\pi/3)$ in the rising half wave and decreases from $f_{\max}$ to $f_{\min}$ in the falling half wave. The solution described by the formula (15) with the minus before $\mathrm{cn}(u\,|m)$ begins with the rising half wave, $f(0)=f_{\min}$, and the solution with the plus begins with the falling half wave, $f(0)=f_{\max}$. Forms of the rising and falling half waves are identical within the accuracy of the inversion of x, and their width is $\Delta/\sqrt{c}$. Equation (17) reflects the fact that the number of half waves in

the interval considered should be integer.

One can verify easily that the function $\Delta=\Delta(\beta)$ is monotonically decreasing; $\Delta(\pi/3)=\pi/\sqrt{2};\Delta\to\infty$ as $\beta\to 0$. Hence the number of roots of Eq. (17) equals the integral part of $\sqrt{2c}/\pi$.

The formula (15) gives $f=-1$ for $\beta=\pi/3$. Hence solutions (15) join the first solution (14); bifurcation points are $c=\pi^2M^2/2$. All the bifurcations are supercritical, that is, non-constant solutions branch off into the region $c>\pi^2M^2/2$.

Integrating (15) we obtain the value of the function $f(x)$ averaged over the discharge vessel cross section

$$\langle f\rangle=2\cos(\beta-\pi/3)-2\sqrt{3}\sin\left[\beta+\frac{\pi}{3}\right]\frac{E(m)}{K(m)}\ . \qquad (19)$$

Here $E(m)$ is the complete elliptic integral of the second kind [14].

The dependencies of $\langle F\rangle=c\langle f\rangle$ on c^2 have been calculated by means of this formula and are shown in Fig. 3, line 1 representing the pair of solutions which consist of one half wave (rising or falling), line 2 representing the pair of solutions which consist of two half waves, etc. The dependencies corresponding to the solutions (14) are shown, too. Evidently, Fig. 3 may be considered as the asymptotic representation of the vicinities of points A and B of the current-voltage characteristic schematically plotted in Fig. 2.

Asymptotic behavior of the solutions (15) as $\beta\to\pi/3$ (that corresponds to $c\to\pi^2M^2/2+0$) is

$$f=-1\pm\left[c-\frac{\pi^2M^2}{2}\right]^{1/2}\frac{4\sqrt{15}}{5\pi M}\cos(\pi Mx)+\cdots\ . \qquad (20)$$

This expression describes the solutions in the vicinity of the offshoot points. It shows that the perturbation of the current-density distribution over the electrode surface is harmonic in the vicinity of the offshoot point, its amplitude growing proportionally to $(U-U_i)^{1/2}$. The subsequent evolution of this distribution is illustrated by Fig. 4, where the function $f(x)$ describing the rising half wave is shown. One can see that as the distance from the offshoot point grows (i.e., β decreases) the minimum of the current-density distribution becomes narrower

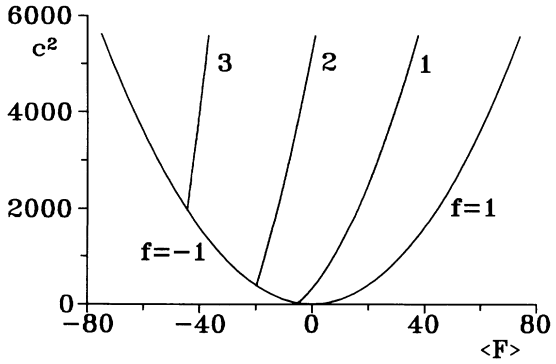

FIG. 3. Asymptotic representation of the current-voltage characteristics in the vicinity of the extreme point, planar case.

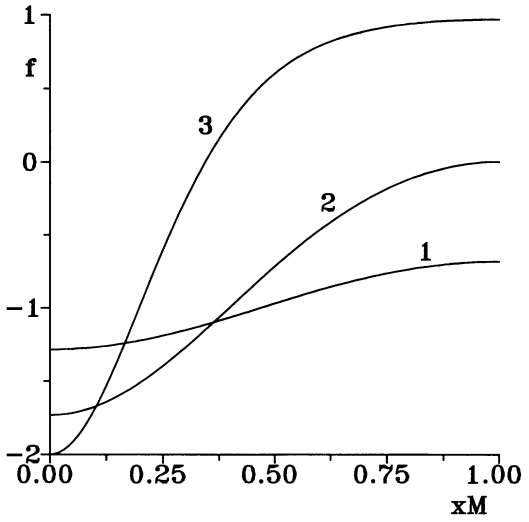

FIG. 4. Perturbations of current-density distribution over the electrode surface, planar case. 1, $\beta=50°$; 2, 30°; 3, 1°.

whereas the width of the maximum grows; in other words, the cold domain begins forming. To obtain an analytical expression describing the shape of this domain at large distances from the offshoot point we apply the limit $\beta\to 0$ $(c/M^2\to\infty)$ to the formula (15) with the minus. The result is

$$f=3\tanh^2\left[\left[\frac{c}{2}\right]^{1/2}x\right]-2\ . \qquad (21)$$

Evidently, far away from the offshoot point the width of the domain is of the order of $L/\sqrt{c}$, the current density in the region occupied by the hot phase equals that corresponding to the point with the same value of U on the ascending part of the one-dimensional current-voltage characteristic, the difference between the current density corresponding to the point of minimum B and the current density in the center of the domain exceeds by a factor of 2 the difference between the current densities corresponding to the point of minimum and to the point with the same value of U on the descending part of the one-dimensional current-voltage characteristic.

V. THE AXISYMMETRIC CASE

Consider now the case when the vessel cross section is a circle and the function f depends on the distance from its center only: $f=f(r)$. The length scale L in this case is taken equal to the radius of the circle.

The problem considered was solved numerically; some results are presented in Figs. 5 and 6. Figure 5 shows the dependencies of $\langle F\rangle$ on c^2, line 1 representing the monotonic solution, lines 2 and 3 representing the solutions which consist of two or three monotonic sections, respectively. Representative graphs of the function f are given in Fig. 6.

It can be shown that in the case considered bifurcation points are $c=p_i^2/2$ (here p_i is the ith positive zero of the Bessel function of the first order). Each nonconstant

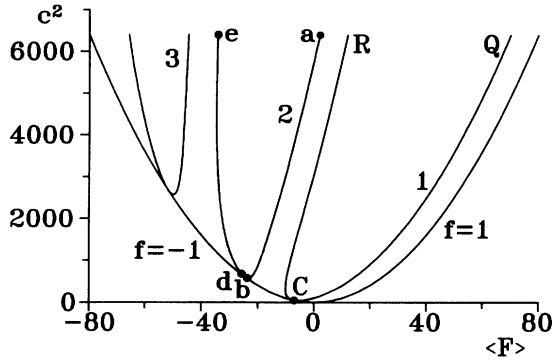

FIG. 5. Asymptotic representation of the current-voltage characteristics in the vicinity of the extreme point, axisymmetric case.

solution consists of two branches, one of them being subcritical (bifurcating into the region $c < p_i^2/2$) and the other supercritical (bifurcating into the region $c > p_i^2/2$); for instance, the branch CQ of line 1 in Fig. 5 is subcritical while the branch CR is supercritical. The subcritical branch corresponds to solutions with the minimum in the center of the circle, the supercritical branch corresponds to solutions with the maximum. The offshoot of current-voltage characteristics in Fig. 5 is smooth, unlike that in Fig. 3 where lines 1–3 branch off from the line $f=-1$ at certain angles.

Asymptotic behavior of solutions in the vicinity of bifurcation points is

$$f=-1+\left[c-\frac{p_i^2}{2}\right]\frac{2J_0^2(p_i)}{p_i^2}\times\left[\int_0^1 rJ_0^3(p_i r)dr\right]^{-1}J_0(p_i r)+\cdots, \qquad (22)$$

where J_0 is the Bessel function of zero order.

Behavior of the solutions as the distance from the bifurcation point grows (i.e., as $c\to\infty$) can be seen from Fig. 6. Cold domains of two types are forming: a central domain which is positioned in the center of the circle, and ring domains which are positioned either inside the circle or at its outer boundary. The current-density perturbation in the central domain is greater than in ring domains: the calculated numerically lower limit value of $f(0)$ is equal to $-3.783\,91$, whereas the lower limit value of the function f in ring domains is equal to -2. Positions of the inner ring domains change as c grows.

The radius of a ring domain substantially exceeds its thickness. Therefore one may expect that its form in the first approximation is the same as the form of a domain in the planar case and is described by the expression (21). However, analytical determination of positions of inner-ring domains is not as simple as determination of domain position in the planar case, when because of spatial uniformity all the distances between neighboring extreme points are equal and do not change as c grows.

As an example, the position of the inner-ring domain is determined in the Appendix for the case when it is the only domain present (such a situation is depicted by line e in Fig. 6). Some asymptotic results [calculated by means of formulas (A3) and (A17)] are presented in Fig. 7 as well as the corresponding results of the numerical solution (line 3 represents the same data as line e in Fig. 6). Agreement between the numerical and asymptotic results is reasonable. It follows from the asymptotic solution that interaction between the domain and the boundaries of the considered region realizes by means of the exponentially small perturbation introduced by the domain into the region occupied by the hot phase.

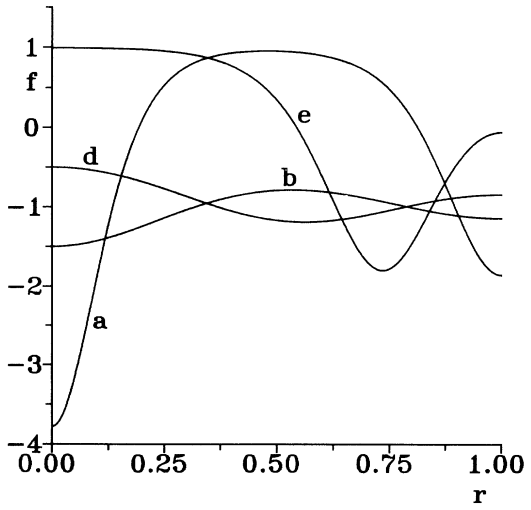

FIG. 6. Perturbations of current-density distribution over the electrode surface, axisymmetric case. States a, b, d, and e are marked in Fig. 5.

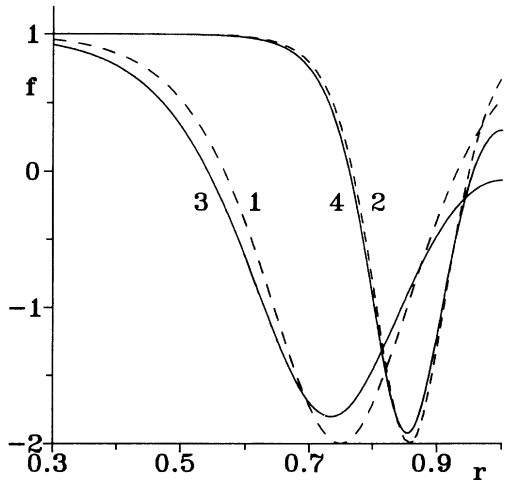

FIG. 7. Perturbations of current-density distribution in the forming ring cold domain. Solid lines, numerical calculation; dashed lines, asymptotic results. Lines $1,3, c=80$; lines $2,4, c=320$.

VI. DISCUSSION OF STATIONARY SOLUTIONS IN THE GENERAL CASE AND THEIR STABILITY

One may hope that main features of the stationary current-density distribution studied above for the planar and axisymmetric cases will be similar in a general case. It may be shown that the bifurcation points at which the nonconstant stationary solutions of the problem (13) branch off from the solution $f=-1$ are connected to the spectrum of the Neumann problem for the two-dimensional Helmholtz equation

$$\Delta_{\parallel}\Phi+k^2\Phi=0\ , \tag{23}$$

where k is the eigenvalue parameter; the region considered, as for Eq. (13), is the cross section of the discharge vessel. We denote by k_i ($i=0,1,2,\ldots$; $k_0=0$; $k_i>0$ for $i\geq 1$) the ith eigenvalue of the problem (23), by N_i the degeneracy of this eigenvalue, and by $\Phi_{im}=\Phi_{im}(x,z)$ ($m=1,\ldots,N_i$) the corresponding orthonormal set of eigenfunctions ($\langle\Phi_{im}\Phi_{jk}\rangle=\delta_{ij}\delta_{mk}$).

Bifurcation points of stationary solutions of the problem (13) correspond to the first and all the following eigenvalues k_i and are $c=k_i^2/2$. Asymptotic behavior of the nonconstant solutions in the vicinity of these points is described by the formulas

$$f=-1+\left[c-\frac{k_i^2}{2}\right]\frac{4}{k_i^2\langle\Phi_{i1}^3\rangle}\Phi_{i1}+\cdots\ , \tag{24}$$

$$f=-1\pm\left[\left[c-\frac{k_i^2}{2}\right]a_i\right]^{1/2}\frac{2}{k_i^2}\Phi_{i1}+\cdots,$$

$$a_i=\left[\sum_{\substack{j=0\\ j\neq i}}^{\infty}\sum_{m=1}^{N_j}\frac{\langle\Phi_{jm}\Phi_{i1}^2\rangle^2}{k_i^2-k_j^2}\right]^{-1}. \tag{25}$$

It is supposed here for the sake of simplicity that $N_i=1$, (24) is written for the case $\langle\Phi_{i1}^3\rangle\neq 0$, and (25) for the case $\langle\Phi_{i1}^3\rangle=0$.

If $\langle\Phi_{i1}^3\rangle\neq 0$ the nonconstant solution consists of subcritical and supercritical branches. If it is not the case, both solutions branching off in the considered bifurcation point are either subcritical (if $a_i<0$) or supercritical ($a_i>0$).

Note that in the planar case $\langle\Phi_{i1}^3\rangle=0$, while in the axisymmetric case $\langle\Phi_{i1}^3\rangle\neq 0$ [accordingly, (24) is in agreement with (22), and (25) with (20)]. Evidently, just this difference results in difference appearances of current-voltage characteristics in Figs. 3 and 5 in the vicinity of bifurcation points.

Solutions considered in Secs. IV and V are valid until the width of the domain is much greater than the layer thickness h. This condition holds in the range $U-U_B\ll U_B$. Obviously, this range is much wider than the range $|U-U_i|\ll\chi^2 U_B$ in which the usual bifurcation theory is applicable to the problem considered [i.e., expressions (20), (22), (24), and (25) are valid].

If the parameter c (which is related to the voltage drop in the near-electrode layer) is considered as fixed, it follows from the general theory [15] that all the stationary solutions of (13) except the second solution (14) are unstable. This means that the transition from the distributed regime to regimes with spots under the conditions of constant voltage drop (in other words, without sufficient ballast resistance) cannot be quasistationary. To analyze stability with ballast resistance the parameter c should be treated as time dependent, its perturbation being subject to the condition of the total voltage drop in the circuit being fixed

$$\frac{\partial}{\partial\tau}(c\langle f\rangle\omega+c^2)=0\ , \tag{26}$$

where ω is the normalized ballast resistance.

Linear analysis of stability of solutions (14) with ballast resistance shows that the second solution (14) is stable. The first solution (14) is unstable if $c>k_1^2/2$; if $c\leq k_1^2/2$, it is stable provided that ballast resistance is sufficient ($\omega>k_1^2$).

Linear analysis of stability of nonconstant stationary solutions in the vicinity of bifurcation points also is an easy matter. Solutions branching off in the second and the following bifurcation points are unstable. In the case $\langle\Phi_{11}^3\rangle\neq 0$ (we suppose $N_1=1$) the subcritical branch of the solution branching off in the first bifurcation point is unstable; the supercritical branch is stable provided that $\omega>k_1^2$. In the case $\langle\Phi_{11}^3\rangle=0$ both solutions branching off in the first bifurcation point are unstable, whether these solutions are subcritical or supercritical.

One can see that, while in the case $\langle\Phi_{11}^3\rangle\neq 0$ only a supercritical solution may be stable, which is the usual situation, in the case $\langle\Phi_{11}^3\rangle=0$, even supercritical solutions branching off in the first bifurcation point cannot be stabilized by the ballast resistance. The reason is that in the case $\langle\Phi_{11}^3\rangle=0$ the ballast resistance affects not only perturbations of the zero-order mode, as in the case $\langle\Phi_{11}^3\rangle\neq 0$, but also of the first order. While its effect on the zero mode is stablilizing, its effect on the first mode contributes to the instability, this instability occurring just in the same moment when the stability against the zero mode is suppressed.

Thus in the conditions of Fig. 3 the transition from the regime with uniform distribution of the current density over the electrode surface (distributed regime) to the regimes corresponding to lines 1,2,3, etc., cannot be carried out in a quasistationary way. In the conditions of Fig. 5 the only quasistationary transition may be that to the branch CR.

It should be emphasized that it does not follow from the above that all the nonconstant stationary solutions which are unstable in the vicinities of bifurcation points will remain unstable far away from these points. In fact, studies of stationary dissipative structures provide contrary examples [16].

VII. ANALYSIS OF NORMAL REGIMES

We shall consider now the theory of normal regimes, when some part of the electrode surface is covered by the hot phase and the other part by the cold phase, a two-dimensional structure (domain wall) separating these

phases. These regimes correspond to section *DE* in Fig. 2.

As the simplest example we treat the stationary planar case when the discharge vessel cross section is a rectangle, its parts adjacent to the lines $x=0$ and 1 being occupied by the cold and hot phases, respectively. The domain wall separating these phases is positioned in the vicinity of the line $x=b$. The value of the voltage drop U is close to U_n (see Fig. 2):

$$U=U_n(1+\varepsilon)\ , \tag{27}$$

where ε is a given parameter, $|\varepsilon|\ll 1$. One of our goals is to determine the relationship between ε and b.

Solutions in the regions occupied by the cold and hot phases coincide to the first approximation with the one-dimensional stationary solution $\mathbf{X}^{(1)}(y)$ in points L and P, respectively, and will be denoted by $\mathbf{X}_L(y)$ and $\mathbf{X}_p(y)$. Asymptotic expansion describing the domain wall is

$$\mathbf{X}=\mathbf{X}_3(\lambda,y)+\varepsilon\mathbf{X}_4(\lambda,y)+\cdots\ , \tag{28}$$

where $\lambda=(x-b)/\sqrt{\chi}$.

The function $\mathbf{X}_3$ obeys the two-dimensional equation

$$\mathbf{B}_3+\nabla\cdot(\mathbf{D}_3\nabla\mathbf{X}_3)=\mathbf{0}\ , \tag{29}$$

where $\mathbf{B}_3=\mathbf{B}(\mathbf{X}_3)$, $\mathbf{D}_3=\mathbf{D}(\mathbf{X}_3)$, and ∇ designates the gradient in the variables λ,y. Boundary conditions for this equation are $\mathbf{X}_3(-\infty,y)=\mathbf{X}_L(y)$, $\mathbf{X}_3(\infty,y)=\mathbf{X}_P(y)$ and mentioned in Sec. II boundary conditions at the electrode surface and at the outer boundary of the considered near-electrode layer (it should be set $U=U_n$).

The stated problem cannot be solved with an arbitrary value of U_n which reflects the well-known fact that phases may coexist only in special circumstances. Thus the condition of solvability of this problem presents the relationship determining U_n (Maxwell's construction; e.g., [17]). To derive an explicit form of this relationship in general is not a simple task, so we present this derivation only for the case when the problem under consideration is scalar. In particular, in such a case the coefficient D may be absorbed by the transformation to the new independent variable $\int D\,dX$ (the so-called heat flux potential), so it will be assumed $D=1$. Also, it will be assumed that mentioned in Sec. II boundary conditions at the electrode surface and at the outer boundary of the considered near-electrode layer either determine the value of the function X (evidently, this value should be independent of x) or specify $\partial X/\partial y$ as a prescribed function of the local X value. Multiply Eq. (29) by $\partial X_3/\partial\lambda$ and write it as

$$B_3\frac{\partial X_3}{\partial\lambda}+\nabla\cdot\left[\frac{\partial X_3}{\partial\lambda}\nabla X_3\right]-\frac{1}{2}\frac{\partial}{\partial\lambda}(\nabla X_3)^2=0\ . \tag{30}$$

Integrate (30) in λ from $-\infty$ to ∞ and in y from 0 to δ (which is the thickness of the near-electrode layer considered). The result may be written as

$$\int_0^\delta\left[\left[\int_{X_L(y)}^{X_P(y)}B(X)dX\right]-\frac{1}{2}\left[\frac{dX_P}{dy}\right]^2+\frac{1}{2}\left[\frac{dX_L}{dy}\right]^2\right]dy=\int_{X_L(0)}^{X_P(0)}\left[\frac{\partial X}{\partial y}\right]_0dX-\int_{x_L(\delta)}^{X_P(\delta)}\left[\frac{\partial X}{\partial y}\right]_\delta dX\ . \tag{31}$$

If the one-dimensional stationary solution $X^{(1)}(y)$ is known, both sides of this relationship may be regarded as known functions of U_n. Thus (31) presents the desired equation determining U_n.

One can see now that analysis of the first approximation allows one to determine the normal voltage drop as well as the form of the domain wall. To determine the position of the domain wall the second approximation should be analyzed.

The asymptotic behavior of the function $\mathbf{X}_3$ at large values of λ is

$$\mathbf{X}_3=\begin{cases}\mathbf{X}_L(y)+w_1\mathbf{U}_L(y)\exp(\alpha_L\lambda)+\cdots\ , & \lambda\to-\infty \quad (32)\\ \mathbf{X}_P(y)+w_2\mathbf{U}_P(y)\exp(-\alpha_P\lambda)+\cdots\ , & \lambda\to\infty \quad (33)\end{cases}$$

where w_1 and w_2 are certain constants of the order of unity; α_L, $\mathbf{U}_L(y)$, α_P, and $\mathbf{U}_P(y)$ are the least positive eigenvalues and corresponding vector eigenfunctions of the eigenvalue problem for the following system of linear ordinary differential equations:

$$\frac{d}{dy}\left[\mathbf{D}_*\frac{d\mathbf{U}_*}{dy}+\mathbf{D}_{1*}\mathbf{U}_*\frac{d\mathbf{X}_*}{dy}\right]+(\mathbf{B}_{1*}+\alpha_*^2\mathbf{D}_*)\mathbf{U}_*=\mathbf{0}\ . \tag{34}$$

Here $*=P,L$; $\mathbf{D}_*=\mathbf{D}(\mathbf{X}_*)$; the matrices $\mathbf{D}_{1*}$ and $\mathbf{B}_{1*}$ are determined similarly to (10), $\mathbf{X}_*$ appearing instead of $\mathbf{X}_B$. Boundary conditions for this equation are the mentioned in Sec. II boundary conditions at the electrode surface and at the outer boundary of the near-electrode layer linearized about $\mathbf{X}_*$ (it should be set $U=U_n$).

The second terms of the asymptotic expansions describing regions occupied by the cold and hot phases also are governed by the problem (34). Choosing solutions which satisfy the condition of matching with the first term of the expansion (28) and the Neumann conditions at the lateral boundaries, one obtains two-term expansions as follows:

$$\mathbf{X}=\mathbf{X}_L(y)+2w_1\exp\left[-\frac{\alpha_L b}{\sqrt{\chi}}\right]\mathbf{U}_L(y)\cosh(\alpha_L v)+\cdots\ , \tag{35}$$

$$\mathbf{X}=\mathbf{X}_P(y)+2w_2\exp\frac{\alpha_P(b-1)}{\sqrt{\chi}}\mathbf{U}_P(y)\times\cosh\left[\alpha_P\nu-\frac{\alpha_P}{\sqrt{\chi}}\right]+\cdots, \tag{36}$$

where $\nu=x/\sqrt{\chi}$.

The second terms of these expansions describe perturbations resulting from the presence of the domain wall. These perturbations contain two components: perturbations directly introduced by the domain wall [which are described by the items proportional to $\exp(\alpha_L\nu)$ and $\exp(-\alpha_P\nu)$, respectively] and those reflected by the lateral boundaries [described by the items proportional to $\exp(-\alpha_L\nu)$ and $\exp(\alpha_P\nu)$]. Evidently, the quantities α_L, α_P may be interpreted as the dimensionless inverse attenuation lengths of perturbations. The Neumann boundary conditions used above result in "perfect reflection" of the perturbations by lateral surface of the discharge vessel.

Now we should treat the interaction of the reflected perturbations with the domain wall, which means matching of the second terms of the expansions (35) and (36) with the second term of (28). Asymptotic behavior of the function $\mathbf{X}_4$ as $\lambda\to-\infty$ or $\lambda\to\infty$ is, respectively,

$$\begin{aligned}&\mathbf{X}_4=w_3\mathbf{U}_L(y)\exp(-\alpha_L\lambda)+\cdots,\\&\mathbf{X}_4=w_4\mathbf{U}_P(y)\exp(\alpha_P\lambda)+\cdots,\end{aligned} \tag{37}$$

where w_3 and w_4 are arbitrary constants. Similarly to the constants w_5 and w_6 in the theory developed in the Appendix of a forming ring domain, w_3 and w_4 are linearly dependent and satisfy a relationship similar to (A6),

$$q_Lw_3-q_Pw_4=1, \tag{38}$$

where q_L and q_P are certain constants of the order of unity.

If b is not close to $\alpha_P/(\alpha_L+\alpha_P)$, reflected perturbations coming to the domain wall from the regions occupied by the cold and hot phases are of different orders of magnitude. Hence only one of them (the larger) may be matched with $\mathbf{X}_4$, while the smaller should be matched with the higher-order term. One obtains for the cases $b<\alpha_P/(\alpha_L+\alpha_P)$ and $b>\alpha_P/(\alpha_L+\alpha_P)$, respectively,

$$w_4=0,\quad w_3=\frac{1}{q_L},\quad \varepsilon=q_Lw_1\exp\left[-\frac{2\alpha_Lb}{\sqrt{\chi}}\right]; \tag{39}$$

$$w_3=0,\quad w_4=-\frac{1}{q_P},\quad \varepsilon=-q_Pw_2\exp\left[\frac{2\alpha_P(b-1)}{\sqrt{\chi}}\right]. \tag{40}$$

In the case $|b-\alpha_P/(\alpha_L+\alpha_P)|\le O(\sqrt{\chi})$ reflected perturbations are of the same order, second terms of both expansions (35) and (36) may be matched with the second term of (28). ε may be written as

$$\varepsilon=q_Lw_1\exp\left[-\frac{2\alpha_Lb}{\sqrt{\chi}}\right]-q_Pw_2\exp\left[\frac{2\alpha_P(b-1)}{\sqrt{\chi}}\right]. \tag{41}$$

Both items in the right-hand side of (41) are of the same order in this case. In other cases one item is negligible and this expression turns into the last formula (39) or (40). Thus (41) is uniformly valid (may be used in all cases).

The asymptotic solution is complete now. In particular, expression (41) is obtained; it relates the position of the domain wall and the difference $U-U_n$. When $0<b<1$, that is, when areas occupied by both phases are comparable, this difference is exponentially small. That means that the corresponding section of the current-voltage characteristic (section DE in Fig. 2) must be close to the horizontal line $U=U_n$ even if the ratio of the layer thickness to the longitudinal dimension is not too small. Numerical results [11] confirm this conclusion: the current-voltage characteristic of a thermally constricted discharge has a distinct flat section already when the corresponding ratio is equal to 0.5.

As it should be expected, as $b\to0$ (or $b\to1$), i.e., when the greater part of the electrode surface is covered by the hot (cold) phase, the order of magnitude of $|\varepsilon|$ tends to unity. This situation corresponds to the vicinities of points E and D in Fig. 2.

If $\varepsilon=0$, to the first approximation $b=\alpha_P/(\alpha_L+\alpha_P)$. In other words, areas occupied by the hot and cold phases when $U=U_n$ are determined by the inverse attenuation lengths α_L and α_P only, namely, each area is proportional to the corresponding attenuation length.

It should be emphasized that, as is also true in the case of the forming ring domain treated in the Appendix, interaction between the non-one-dimensional structure (domain wall) and the lateral boundaries occurs by means of perturbations introduced by the domain wall into regions occupied by the cold and hot phases, this interaction being described by exponentially small terms.

VIII. CONCLUDING DISCUSSION

The above theory provides an asymptotic description of stationary non-one-dimensional solutions in the vicinities of the offshoot points (points C and F in Fig. 2) and in normal regimes (corresponding to the line DE).

Offshoot of stationary non-one-dimensional solutions occurs in the vicinities of extreme points of the one-dimensional current-voltage characteristic. Perturbation of the current density along the electrode surface in this vicinity is governed by Eq. (13). Its derivation has many features in common with the derivation of the Ginzburg-Landau equation in a vicinity of an instability point of reaction-diffusion systems [17,18], however (13) is the Fisher equation rather than the Ginzburg-Landau one. This question is interesting by itself, but we only note here that it is due to the fact that we are dealing with structures with slow variation in space and time. The other difference is that the considered system is of strongly different dimensions, so the number of space variables

in (13) is less than in the initial problem.

In [9] small deviations from the one-dimensional references state were considered in the framework of equations similar to (2)–(4). This approach agrees with that used in Sec. III, however, the resulting equation in [9] differs from (13). For example, the term with $\Delta_{\|}$ in the equation in [9] accounts only for diffusion of the charged particles; if diffusion is neglected as compared to drift, this term in treatment [9] vanishes, in contrast to that of Sec. III. This difference results from a number of assumptions used in [9], in particular, that of quasineutrality of perturbations.

It is worth noting that the question of whether diffusion of charge particles plays a decisive role in formation of structures on the cathode of the glow discharge has been intensively discussed (e.g., [19] and references therein). Present results are on the line of [6,20]: in principle, structures may appear without diffusion, due to only nonquasineutrality and drift.

Solutions to Eq. (13) studied in Secs. IV–VI describe evolution of perturbations from harmonic to spotlike. Consider conclusions which follow in regard to the transition between the normal and abnormal regimes, i.e., between sections *DE* and *BN* in Fig. 2.

This transition cannot be continuous: line *DE* does not reach line *BN*. If the transition is quasistationary, it should occur along the path *EFB* and be accompanied by the change of the voltage drop. At least some part of this path, in principle, may be passed in a quasistationary way. Then, the point separating regimes with uniform and nonuniform current-density distributions (point *F*) is positioned on the descending section of the current-voltage characteristic. The exact position of this point depends on the dimensions of the cross section of a discharge vessel. The features of joining the current-voltage characteristics corresponding to the regimes with uniform current-density distribution and nonuniform one (*BF* and *FE*, respectively) depend on the shape of the cross section. For instance, if the cross section is a sector of a circle with the angle at the apex, say, 60° (such that the axisymmetric solution is the first to branch off), the initial portion of the characteristic corresponding to the nonuniform discharge will be represented by the branch *CR* in Fig. 5. It is interesting to note that the slope of this branch to the current axis is positive, while those of sections *DE* and *FB* in Fig. 2 are negative. In other words, the section *DEFB* is *Z* shaped.

Generally speaking, the relaxation time of the discharge in the near-electrode layer is equal to the characteristic time t^0 introduced in Sec. II, which may be interpreted as the time of spreading of perturbations across the layer. However, the relaxation time in regimes near point *B* (for example, the time of a spontaneous transition from section *BF* to section *ED*) is by a factor χ^{-1} greater and equal to the time of perturbation spreading in the direction along the surface. On the other hand, it follows from the analysis of Sec. VII that the relaxation time in normal regimes is of the order of t^0.

Consider now the applicability of the presented results to the glow-discharge near-cathode region. These results were derived using the Neumann (no-flux) boundary conditions at the lateral surface of the discharge vessel, which means neglect of the losses of the charged particles due to diffusion to the lateral surface. In fact, because of these losses the current distribution over the cathode surface is nonuniform even in abnormal regimes: the current density is reduced in small regions adjacent to the lateral surface. The width of this region is of the order of $h[kT_e/(eU)]^{1/2}$, where kT_e is the average energy of electrons.

At low pressures $kT_e/(eU)$ is of the order of unity. When the current in the normal regime is increased, the cold domain formed at point *E* cannot vanish and section *EF* will be absent. Thus one may expect that at low pressures the above-discussed features may be present only if diffusive losses to the lateral surface are excluded or, at least, considerably reduced.

This conclusion is supported by the experiment [21] in which the main discharge was surrounded by the auxiliary one. Stationary states corresponding to sections *DE* and *BP* were observed. The transition between these sections was nonstationary and with hysteresis. Note that the variation of the voltage drop corresponding to this transition (i.e., the difference between the normal voltage drop and the voltage drop corresponding to the minimum point *B*) amounted only to a few volts.

It seems interesting to measure the characteristic time of this transition and to compare it with the relaxation time in normal or abnormal regimes: while the latter may be expected to be of the order of the time of ion drift across the layer, the former is expected to be larger by a factor of χ^{-1}. Another very interesting question is whether it is possible to stabilize section *BF* in experiments of this type (that is, with an auxiliary discharge). If the answer is positive, one can think of further experimental investigations (maybe, with a number of neighboring discharges) in order to realize the stationary solutions of the above-discussed type, current-voltage characteristics with a break point being of particular interest.

With increasing pressure relatively more electrons have low energies [22] and it may be possible that the average energy becomes small as compared to eU. Thus it seems interesting to investigate experimentally the transition between normal and abnormal regimes also at high pressures: if the transition occurs discontinually without an auxiliary discharge, it means that the ratio $kT_e/(eU)$ is small and diffusion is not important as compared to drift.

ACKNOWLEDGMENTS

The author appreciates Processor G. Ecker's and Professor K. G. Müller's helpful discussions. This work was performed within the activities of the Sonderforschungsbereich 191 of the Deutsche Forschungsgemeinschaft and was supported by the Alexander von Humboldt-Stiftung.

APPENDIX

Denote the coordinate of the peak of the domain by *R*. Considering *c* as the large parameter we seek the asymptotic expansion valid in the vicinity of the point $r=R$ as

$$f(r;c)=f_1(\rho)+\frac{1}{\sqrt{c}}f_2(\rho)+\cdots\ ,\quad \rho=(r-R)\sqrt{c}\ . \tag{A1}$$

The function f_1 satisfies

$$\frac{d^2f_1}{d\rho^2}-f_1^2+1=0\ ,\qquad \frac{df_1}{d\rho}(-\infty)=\frac{df_1}{d\rho}(0)=\frac{df_1}{d\rho}(\infty)=0\ . \tag{A2}$$

The solution of this problem is similar to (21),

$$f_1=3\tanh^2\left[\frac{\rho}{\sqrt{2}}\right]-2\ . \tag{A3}$$

The function f_2 satisfied the equation

$$\frac{d^2f_2}{d\rho^2}-2f_1f_2=-\frac{1}{R}\frac{df_1}{d\rho}\ . \tag{A4}$$

The asymptotic behavior of solutions of this equation (which is necessary for the following matching) is as follows:

$$f_2=w_5\exp(-\sqrt{2}\rho)+\cdots,\quad \rho\to-\infty \qquad f_2=w_6\exp(\sqrt{2}\rho)+\cdots,\quad \rho\to\infty \tag{A5}$$

where w_5 and w_6 are arbitrary constants. Multiplying (A4) by $df_1/d\rho$ and integrating we obtain the relationship between these constants

$$w_5-w_6=\frac{1}{5\sqrt{2}R}\ . \tag{A6}$$

To describe the range $0<r<R$ we introduce the two-scale asymptotic expansion

$$f(r;c)=1+f_3(\xi,\eta)+\cdots\ . \tag{A7}$$

Here $\xi=r\sqrt{c}$ and $\eta=r$ are the fast and slow variables, respectively; $|f_3|\ll 1$.

The function f_3 obeys the equations

$$\frac{\partial^2f_3}{\partial\xi^2}-2f_3=0,\quad \frac{\partial f_3}{\partial\xi}+2\eta\frac{\partial^2f_3}{\partial\xi\partial\eta}=0\ . \tag{A8}$$

The solution is

$$f_3=\frac{C_1}{\sqrt{\eta}}\exp\sqrt{2}\xi+\frac{C_2}{\sqrt{\eta}}\exp(-\sqrt{2}\xi)\ , \tag{A9}$$

where C_1 and C_2 are arbitrary constants.

This solution has a singularity at $r=0$. That is why for small r a new asymptotic expansion should be introduced:

$$f(r;c)=1+f_4(\xi)+\cdots\ . \tag{A10}$$

The function f_4 is asymptotically small ($|f_4|\ll 1$) and satisfies the equation and the boundary condition as follows:

$$\frac{1}{\xi}\frac{d}{d\xi}\left[\xi\frac{df_4}{d\xi}\right]-2f_4=0,\quad \frac{df_4}{d\xi}(0)=0\ . \tag{A11}$$

The solution may be expressed in terms of the modified Bessel function of zero order I_0,

$$f_4=C_3I_0(\sqrt{2}\xi)\ , \tag{A12}$$

where C_3 is an arbitrary constant.

Matching leading terms of the expansions (A7) and (A10) with the known asymptotic behavior of the function I_0 at large values of the argument we find the relationship between the constants C_1 and C_3:

$$C_1=C_3(2\pi\sqrt{2c})^{-1/2}\ . \tag{A13}$$

Evidently, $C_2=O(C_1)$.

Matching leading terms of the expansion (A7) [that is, the first term in the right-hand side of (A7) and the first term in the right-hand side of (A9)] with the first term of the expansion (A1) we find the constant C_1:

$$C_1=-12\sqrt{R}\exp(-\sqrt{2c}R)\ . \tag{A14}$$

The second term in the right-hand side of (A9) is of the order of $\exp(-\sqrt{8c}R)$ as $r\to R$ and cannot be matched with the second term of the expansion (A1). Therefore it should be supposed that $w_5=0$.

Asymptotic expansion which is valid in the region between the domain and the outer boundary of the circle is similar to (A7),

$$f(r;c)=1+f_5(\xi,\eta)+\cdots\ ,\qquad f_5=\frac{C_4}{\sqrt{\eta}}\exp\sqrt{2}\xi+\frac{C_5}{\sqrt{\eta}}\exp(-\sqrt{2}\xi)\ , \tag{A15}$$

where C_4 and C_5 are arbitrary constants, and $|f_5|\ll 1$.

Taking into account that $\partial f_5/\partial\xi$ equals zero at $r=1$ and matching expansions (A1) and (A15) we find C_4 and C_5 and obtain the equation determining the parameter R,

$$C_4=-12\sqrt{R}\exp[\sqrt{2c}(R-2)]\ ,\qquad C_5=-12\sqrt{R}\exp\sqrt{2c}R\ , \tag{A16}$$

$$\exp[\sqrt{8c}(1-R)]=60R\sqrt{2c}\ . \tag{A17}$$

Now the asymptotic solution is complete. The physical sense of results is quite clear. The expansion (A1) describes the domain. As was expected, the form of the domain differs from that in the planar case only in the second approximation which is of the order of $1/\sqrt{c}$. However, this approximation should be analyzed to determine the position of the domain. It may be seen from Eq. (A17) that the distance between the peak of the domain and the boundary of the circle is of the order of $L(\ln c)/\sqrt{c}$ and exceeds substantially the domain width which is of the order of $L/\sqrt{c}$. That means that the domain moves to the boundary of the circle as c grows, however its width decreases faster than the distance to the boundary. Accordingly, the current-density distribution in the domain becomes closer to (21).

The expansions (A7) and (A10) describe the solution in the region surrounded by the domain. This region is occupied by the cold phase. The perturbation due to the domain presence which is described by the second terms of the expansions decreases in this region from the values

of the order of unity in the domain to the exponentially small [of the order of $\sqrt{c}\exp(-\sqrt{2c})$] value in the center of the circle.

The expansion (A15) describes the solution in the region between the domain and the boundary of the circle. This region is occupied by the hot phase, too. The order of magnitude of the perturbation introduced by the domain presence decreases here from unity in the domain to $c^{-1/4}$ at the boundary.

---

*Permanent address: Institute for High Temperatures of the USSR Academy of Sciences, Izhorskaya, 13/19, Moscow 127412, U.S.S.R.

[1] D. G. Boyers and W. T. Tiller, J. Appl. Phys. **44**, 3102 (1973).

[2] D. G. Boyers and W. T. Tiller, Appl. Phys. Lett. **41**, 28 (1982).

[3] Ch. Radehaus, T. Dirksmeyer, H. Willebrandt, and H.-D. Purwins, Phys. Lett. A **125**, 92 (1987).

[4] K. G. Müller, Phys. Rev. A **37**, 4836 (1988).

[5] S. W. Simpson and C. A. Schmidt-Harms, Appl. Phys. Lett. **52**, 1950 (1988).

[6] M. S. Benilov, Zh. Tekh. Fiz. **58**, 2086 (1988) [Sov. Phys.—Tech. Phys. **33**, 1267 (1988)].

[7] H.-D. Purwins, C. Radehaus, T. Dirksmeyer, R. Dohmen, R. Schmeling, and H. Willebrandt, Phys. Lett. A **136**, 480 (1989).

[8] H. Willebrandt, C. Radehaus, F.-J. Niedernostheide, R. Dohmen, and H.-D. Purwins, Phys. Lett. A **149**, 131 (1990).

[9] C. Radehaus, R. Dohmen, H. Willebrandt, and F.-J. Niedernostheide, Phys. Rev. A **42**, 7426 (1990).

[10] H. Willebrandt, F.-J. Niedernostheide, E. Ammelt, R. Dohmen, and H.-D. Purwins, Phys. Lett. A **153**, 437 (1991).

[11] M. S. Benilov and N. V. Pisannaya, Zh. Tekh. Fiz. **58**, 2075 (1988) [Sov. Phys.—Tech. Phys. **33**, 1260 (1988)].

[12] E. A. Coddington and N. Levinson, *Theory of Ordinary Differential Equations* (McGraw-Hill, New York, 1955).

[13] J. D. Murray, *Mathematical Biology,* Biomathematics Vol. 19 (Springer, Berlin, 1989).

[14] *Handbook of Mathematical Functions,* edited by M. Abramowitz and I. A. Stegun (Dover, New York, 1964).

[15] P. C. Five, *Mathematical Aspects of Reacting and Diffusing Systems,* Lecture Notes in Biomathematics Vol. 28 (Springer, Berlin, 1979).

[16] G. Nicolis and I. Prigogine, *Self-Organization in Nonequilibrium Systems* (Wiley, New York, 1977).

[17] H. Haken, *Synergetics, An Introduction,* Springer Series in Synergetics Vol. 1 (Springer, Berlin, 1978).

[18] Y. Kuramoto, *Chemical Oscillations, Waves, and Turbulence,* Springer Series in Synergetics Vol. 19 (Springer, Berlin, 1984).

[19] Yu. P. Raizer and S. T. Surgikov, Teplofiz. Vys. Temp. **26**, 428 (1988) [High Temp. **26**, 304 (1988)].

[20] S. Hollo and B. Nyiri, in *Contributed Papers of XX International Conference on Phenomena in Ionized Gases (Il Ciocco, 1991),* edited by V. Palleschi and M. Vaselli, (IFAM, Pisa, 1991), Vol. 2, p. 482.

[21] L. Rothhardt, in *Proceedings of the 5th International Conference on Ionization Phenomena in Gases (Munich, 1961)* (North-Holland, Amsterdam, 1962), Vol. 1, p. 290.

[22] G. Francis, in *Gas Discharges,* edited by S. Flügge, Encyclopedia of Physics Vol. XXII (Springer, Berlin, 1956), p. 53.